2026-01-0458 Published 07 Apr 2026

Behavioral Determinants of Electric Vehicle Battery Degradation: Evidence from Large-Scale Real-world Operations

Tianyi Liu, Hao Jing, Jiankuan Zhu, Yongjian Chen, and Shiqi Ou South China University of Technology

Xiaodong Qian Wayne State University

Citation: Liu, T., Jing, H., Zhu, J., Chen, Y. et al., "Behavioral Determinants of Electric Vehicle Battery Degradation: Evidence from Large-Scale Real-world Operations," SAE Technical Paper 2026-01-0458, 2026, doi:10.4271/2026-01-0458.

Received: 18 Nov 2025 Revised: 17 Dec 2025 Accepted: 21 Jan 2026

Abstract

Electric vehicles (EVs) are central to sustainable transport, yet battery service life remains a limiting factor for cost and adoption. Distinct from traditional laboratory-based simulations that often fail to capture the complexity of field conditions, this study investigates how EV user behavior—including driving style and charging demands—influences capacity using large-scale, real-world operational data from daily EV usage. A data-driven framework is developed to quantify driving and charging behaviors through multidimensional feature extraction at the vehicle level and estimate battery State-of-Health (SOH) trajectories, enabling direct linkage between individual behavior patterns and degradation outcomes. Results reveal substantial heterogeneity in aging rates explicitly driven by diverse user behaviors: under identical urban conditions, vehicles with a radical driving style exhibit approximately 81% faster SOH decline per 20,000 km than those with a moderate style; regarding charging intensity, in controlled comparison scenarios, increasing fast-charge counts from the baseline interval of 90–120 to the elevated interval of 150–180 is associated with a ~2.1% reduction in median SOH when holding other factors constant; and similarly, increasing deep charge–discharge events from 160–180 to 220–240 corresponds to an additional ~2.0–2.3% cumulative SOH loss. These findings quantify the behavioral determinants of capacity fade in the field and demonstrate that aggressive driving, frequent fast charging, and deep discharge habits materially accelerate battery degradation. The framework provides actionable evidence for adaptive charging guidance and personalized driving strategies, extending battery longevity and enhancing the sustainability of electric mobility systems.

Keywords

Battery degradation, Electric vehicle, Real-world operational data, State of health, Using behavior

Introduction

Electric vehicles (EVs) have significant potential to reshape the global energy landscape and substantially reduce carbon emissions [1]. Their growing prominence in the international market is clearly reflected in the rapid expansion of global EV sales in recent years [2]. As reported in the International Energy Agency's (IEA) Global EV Outlook 2025, EV adoption is expected to reach parity with internal combustion engine vehicles by 2030, with projected sales of approximately 20 million units in 2025, accounting for over one-fourth of all vehicle sales worldwide [3]. These developments underscore the emergence of EVs as a mainstream transportation solution for the future. Nevertheless, the rapid growth and popularity of EVs are tempered by persistent challenges, with State-of-Health (SOH) and energy density of lithium-ion batteries remaining key bottlenecks to EV adoption [4,5]. SOH represents a key indicator of a battery's condition relative to its nominal performance, typically expressed as a percentage. It reflects the remaining capacity, efficiency, and overall functionality of the battery compared to its initial state. Over time, the SOH of EV batteries inevitably declines due to cyclic aging, temperature fluctuations, and mechanical or electrochemical stress [6]. Importantly, the actual SOH evolution and driving range of EVs are not solely determined by cell design or manufacturing quality but are strongly influenced by the complex

and dynamic conditions encountered during real-world operation [7]. Therefore, systematically analyzing large-scale field data to investigate the influence of behavioral factors on battery SOH is essential for understanding real-world degradation patterns and informing strategies to improve EV reliability and performance.

In the study of battery SOH degradation for EVs, early research predominantly relied on laboratory-based simulations under controlled operating conditions. Experimental evidence indicates that, at the mechanistic level, lithium-ion battery degradation is governed by a set of interrelated electrochemical processes, including the growth of the solid electrolyte interphase (SEI), lithium plating, cathode particle cracking, and electrolyte decomposition. These processes act synergistically, leading to a continuous decline in usable capacity and a pronounced increase in internal resistance, thereby accelerating the overall deterioration of performance [8]. Accelerated aging tests in laboratory settings have provided systematic elucidation of these degradation pathways. For example, findings indicate that operating temperatures exceeding 40°C or deep-discharge cycles can reduce cycle life by approximately 50% [9]. However, such controlled tests present significant limitations, and their results often overestimate field-observed degradation rates by about 20%–40%. This overestimation arises primarily because laboratory conditions cannot fully reproduce the dynamic aspects of real-world EV operation, such as partial cycling, fluctuating load profiles, and complex driving scenarios, which may, in certain cases, mitigate or alter aging rates [10]. Field investigations have substantiated these observations, revealing that under mixed operational conditions, the average annual capacity fade rate is about 1.8%. Variations in ambient temperature contribute to an estimated 20–30% difference in degradation rates across geographic regions [11]. In real-world operations, batteries typically exhibit an annual degradation of 1.8–2.3%, often following a non-linear trajectory characterized by an initial rapid drop followed by a stabilization phase, which contrasts sharply with the linear projections derived from controlled laboratory tests [12]. This substantial discrepancy highlights a critical limitation: conventional laboratory protocols, which rely on constant current cycling, fail to capture the stop-and-go dynamics of urban driving and the heterogeneity of user charging behavior. These dynamic operational and usage patterns can exert varying degrees of influence on SOH degradation [13, 14].

Building upon these findings, a critical subset of real-world operational variability arises from user-specific behaviors, which can amplify, mitigate, or otherwise modulate battery degradation pathways depending on driving, charging, and usage patterns. User behaviors—including aggressive acceleration, irregular charging, and temporal usage patterns—further modulate these effects, introducing variability that can accelerate SOH decline by 15–30% under high-stress conditions [15]. Without targeted analysis of such heterogeneous factors from large-scale telematics data, strategies to mitigate battery degradation remain underdeveloped, thereby limiting EV sustainability. User-specific behaviors exert a profound influence on battery SOH. Driving style dictates current demand patterns, with aggressive behaviors—characterized by frequent hard accelerations (>2 m/s^2) and decelerations—elevating root-mean-square currents and promoting lithium plating, which can accelerate capacity fade by 15–30% over 50,000 km compared to conservative driving [16.17]. Interestingly, real-world telematics from urban fleets indicate that dynamic stop-and-go cycles, often associated with aggressive driving, can paradoxically extend battery life by up to 40% compared to steady laboratory cycling. However, excessive energy throughput still correlates with higher fade rates [18,19]. Charging behavior compounds these risks: fast charging (>50 kW) introduces thermal stress and lithium plating, leading to 10–25% faster SOH decline. At the same time, irregular state-of-charge swings during peak-hour usage exacerbate pack-level inconsistencies [20]. Temporal patterns, such as morning commutes during high-traffic periods, further intensify these effects by aligning high-load periods with suboptimal thermal conditions, as evidenced by large-scale usage analyses [21]. Table 1 summarizes the research process for the SOH of EV batteries.

The existing literature has progressively uncovered the influence of real-world operational factors—ranging from regional differences in ambient temperature to variability in user driving and charging behaviors—on EV battery SOH degradation. These studies have contributed valuable empirical evidence, yet important gaps remain. In particular, most analyses are conducted at an aggregated fleet level, overlooking heterogeneous user-specific patterns that may shape degradation pathways. Moreover, causal assessments seldom integrate multiple behavioral dimensions (e.g., charging depth, charging duration) with fine-grained SOH measurements. To overcome these limitations, this study develops a comprehensive, data-driven analytical framework that captures the impacts of individual real-world user behaviors on EV battery health. The framework utilizes large-scale telematics data from the Guangzhou New Energy Vehicle Data Platform to identify nuanced degradation patterns, as illustrated in Figure 1. In addition, the innovations of this work are summarized as follows:

1. Large-scale real-world validation: Using a unified dataset of over twenty million operational

TABLE 1 Comparison of Battery Degradation Research

Research Type	Key Method	User Behavior	Gaps
Lab Studies	Controlled aging tests [7, 8, 9]	Not Considered	Overestimated degradation, lacks real-world fidelity [10,13,14].
Field Studies	Macro-scale fade data analysis [11,12]	Indirectly Linked	Fails to quantify the impact of specific user behaviors [15].
User Behavior Studies	Fleet telematics analysis [15, 16, 17, 18, 19, 20, 21]	Directly Analyzed	Limited studies, lack of mining of large-scale heterogeneous behavior data [16]

FIGURE 1 Research framework.

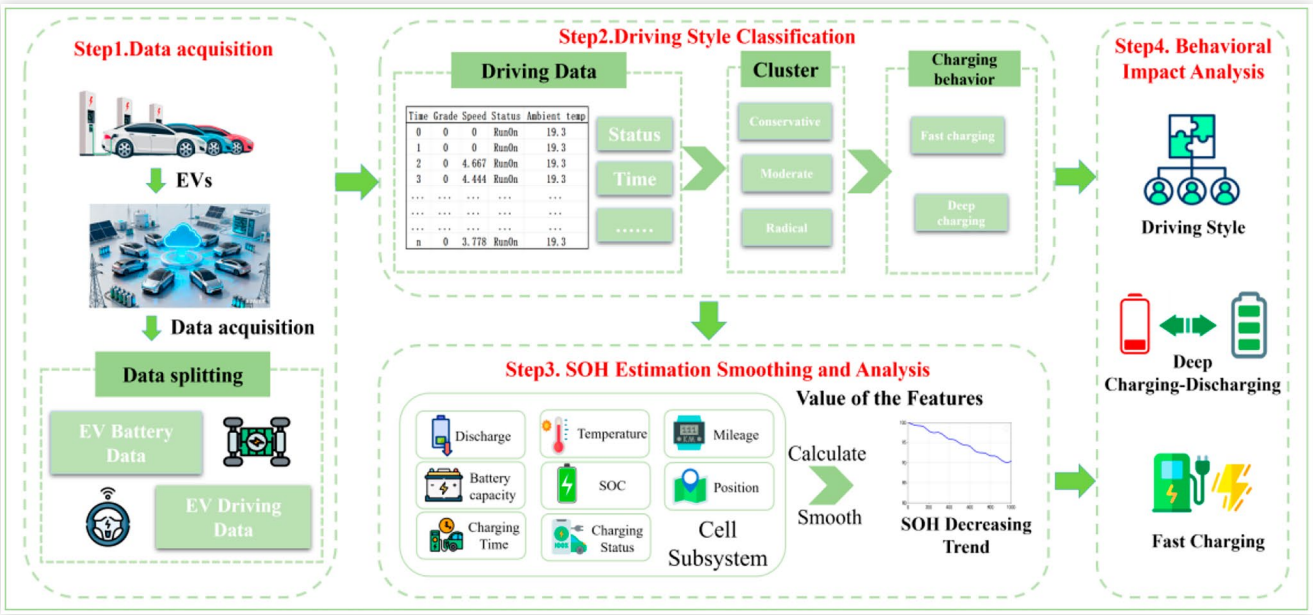

records, this study performs a comprehensive empirical evaluation of EV battery degradation, bridging the gap between laboratory findings and field performance.

2. Integration of behavioral profiling and battery degradation modeling: This study quantitatively links user-specific driving and charging patterns with long-term SOH evolution, revealing causal behavior degradation relationships under real-world conditions.
3. Multi-factor analysis of degradation drivers: The analysis simultaneously considers driving style and charging behavior, enabling a holistic understanding of how behavioral and environmental factors jointly influence SOH trajectories.

The remainder of this paper is organized as follows. Section 1 outlines the research background and motivation. Section 2 describes the data sources, metadata characteristics, and end-to-end preprocessing pipeline. Section 3 details the methodology for characterizing driving style and estimating battery SOH. Section 4 reports and interprets the empirical results, quantifying the marginal and joint effects of user driving and charging behaviors on SOH degradation. Section 5 summarizes the principal findings and discusses implications for battery longevity management and future research.

Data Description and Pre-Processing

Data Description

The empirical analysis in this study is based on large-scale real-world data collected from EVs under actual operating conditions. It comprises data from seven battery EVs of the same vehicle model in Guangzhou, totaling approximately 15 million records over one year. Each vehicle is sampled at 10-second intervals, with more than 70 recorded parameters, including timestamp, vehicle-level data, motor performance, battery information, and vehicle speed. To avoid memory overflow and excessive computational time caused by high-dimensional data, only 11 variables that are closely related to SOH are retained: timestamp, vehicle speed, charging status, accumulated mileage, total voltage, total current, State-of-Charge (SOC), minimum cell voltage, maximum cell voltage, minimum cell temperature, and maximum cell temperature. These variables are specifically selected based on domain knowledge of lithium-ion battery electrochemistry and vehicle dynamics. For instance, cell voltage extremes and temperature are direct indicators of changes in internal resistance and thermal stress. At the same time, speed and current profiles capture the kinetic load applied to the battery pack. This selection ensures that the dataset retains the most critical features governing degradation mechanisms while reducing computational redundancy. The specific data after screening are shown in Table 2.

The laboratory environment provides highly stable and undisturbed conditions for battery testing, enabling testing under strictly controlled conditions. However, the sensor data from the vehicles is more susceptible to complex, multi-source environmental factors, including meteorological conditions, surrounding infrastructure, and interference during data collection and transmission. These factors collectively lead to instability in the quality of data uploaded to cloud platforms at different times and under various conditions. Figure 2 shows the partial data information statistics of the vehicles involved in this experiment. Laboratory testing typically covers the entire SOC cycle range, from 0% to 100%, to comprehensively characterize the performance and degradation behavior

TABLE 2 Summary of Key Variables for Relating Battery Degradation.

Field Name	Unit	Description
$Time_{sample}$	s	Timestamp representing the precise recording time within the day.
$Mileage_{total}$	km	Total mileage traveled by the vehicle
Speed	km/h	Vehicle longitudinal speed measured from the chassis CAN bus.
$V_{battery}$	V	Total voltage of the battery pack.
$I_{battery}$	A	Battery current.
$V_{battery\_max}$	V	The maximum battery pack voltage.
$V_{battery\_min}$	A	The minimum voltage of the battery pack.
$Temp_{battery}$	°C	Battery pack temperature during sampling.
SOC	%	State-of-Charge estimated by the BMS.
$Status_{charging}$	—	Charging status flag
$Status_{dcdc}$	—	Status of the DC/DC converter.
Longitude	°	Longitude coordinate.
Latitude	°	Latitude coordinate.

of the battery; However, as shown in Figure 2 (a, b), charging events on actual roads often only occur within a partial SOC range, generally starting from about 30% -40% and ending between 80% -90%. This partial charging mode may affect the long-term evaluation of battery performance. Figure 2 (c, d) illustrates the continuous dynamic changes in voltage and current of the vehicle during operation, highlighting the complexity of the road load curve compared to the constant load in the laboratory, which more closely resembles real-world operating conditions. Regarding the internal characteristics of the battery pack, Figure 2 (e, f) shows the dynamic ranges of cell voltage and cell temperature. It is worth noting that in Figure 2(f), some individual cell voltage readings appear to be around 0 V, which is lower than the physical lower limit of the lithium-ion electrochemical system. This also suggests that sensor errors or data outliers may have occurred during sampling or data transmission. In summary, there are significant differences between on-site data collected by vehicles and laboratory benchmarks, often due to noise, anomalies, and inconsistent records. Before conducting data analysis, strict anomaly detection and data cleaning must be performed on the raw data to ensure data reliability and the validity of the conclusions.

Data Pre-Processing

Unlike laboratory measurements collected under controlled conditions, real-world vehicle telematics are exposed to exogenous disturbances—e.g., weather, urban

FIGURE 2 Raw data distributions for all sampled vehicles.

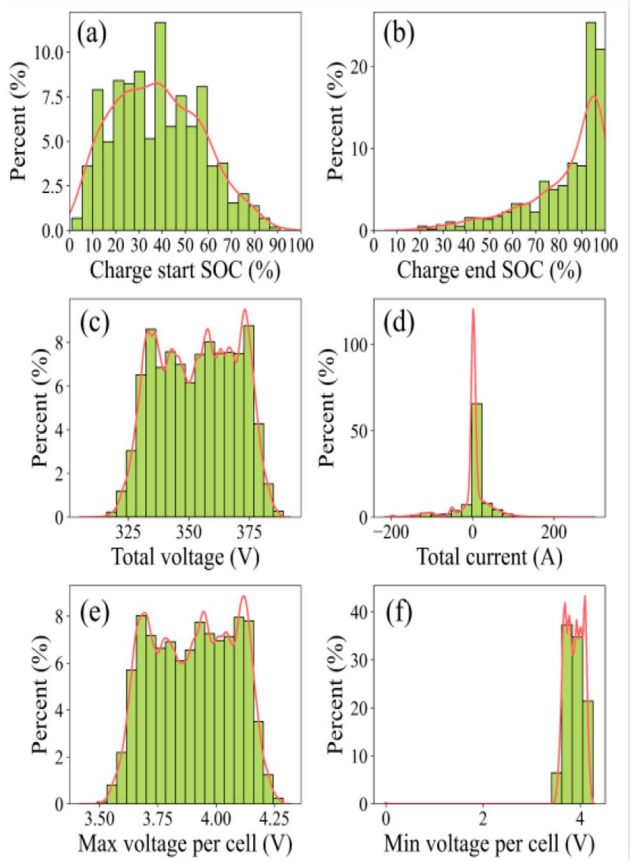

canyons and building shadowing, and telemetry bandwidth limits—which introduce substantial variability in data quality. Consequently, raw uploads to the cloud platform require systematic conditioning before analysis can be performed. This study, therefore, implements a comprehensive cleaning and preprocessing workflow to construct a high-quality dataset suitable for reliable inference.

As shown in Figure 3, the procedure comprises six stages. 1) De-duplication: records are deduplicated by sampling the timestamp. 2) Ambient temperature augmentation: given the strong temperature dependence of battery performance and the large temporal variability in service, historical ambient temperature is retrieved from the China Weather Network using vehicle geolocation and time, then matched to each record. 3) Outlier treatment: outliers are identified via the interquartile range (IQR) criterion and winsorized to the nearest non-outlying boundary. 4) Operational segmentation: data are partitioned into driving, charging, and resting segments based on charging status and speed. Because drive-cycle currents exhibit high ripple and relatively coarse sampling—conditions that bias health feature and label estimation—SOH estimation is performed on charging segments, where current trajectories are smoother and quasi-steady, yielding more accurate SOH inference [22]. 5) Charging-segment screening: to reduce label noise from very short or

FIGURE 3 Flowchart for vehicle data processing.

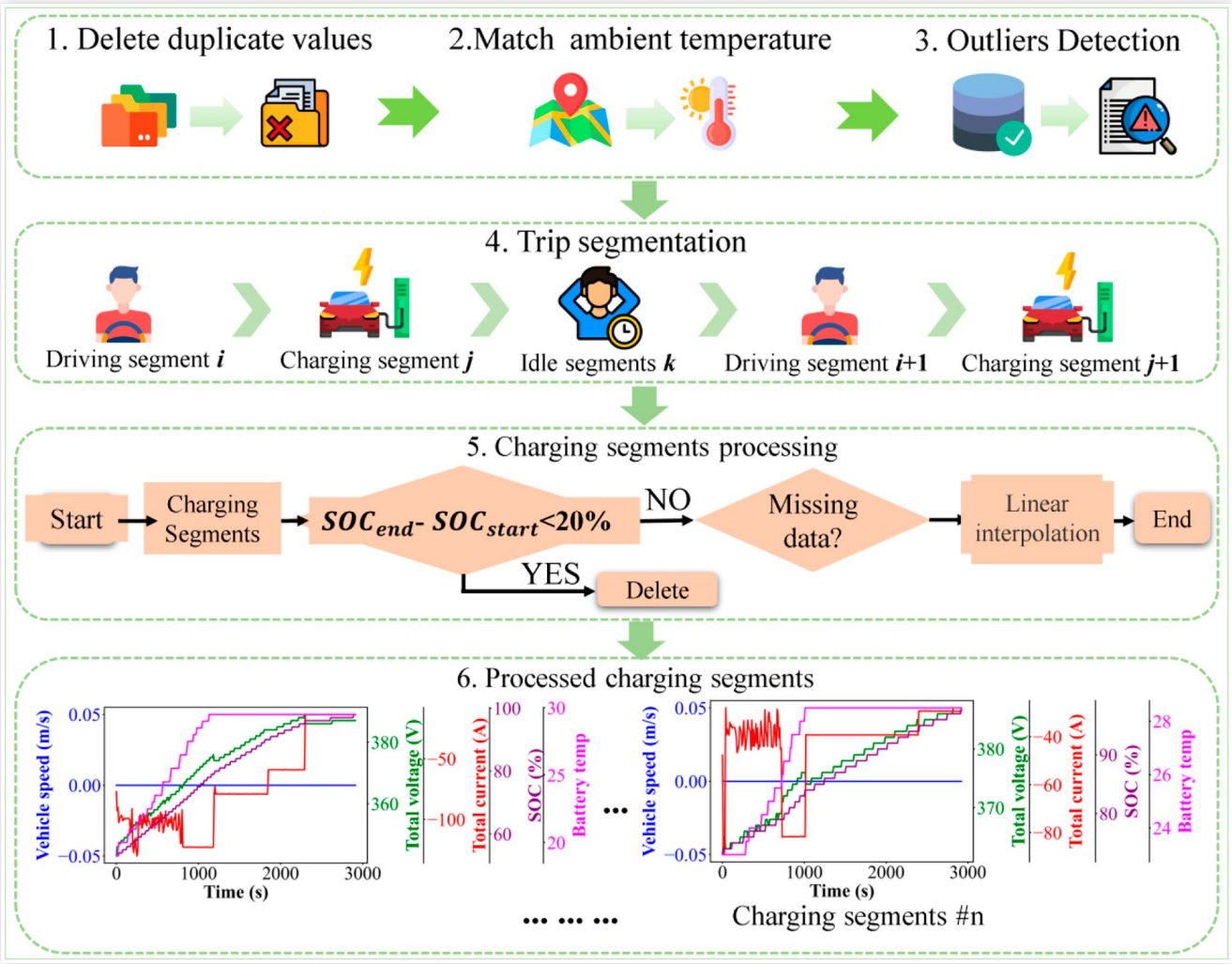

shallow charges, only charging segments with ΔSOC > 20% are retained [23]. 6) Imputation and retention: missing values within retained charging segments are imputed by linear interpolation; driving segments are preserved for subsequent driving-style analysis. The resulting processed fragments constitute the analysis-ready dataset for SOH label calculation and downstream empirical modeling.

Method

Driving Style

To capture the diversity of EV-driving behaviors, this study first conducts a detailed analysis of driving styles using processed real-world driving data. For each vehicle, a comprehensive set of 19 interpretable features is extracted from the cleaned speed time series to characterize the statistical, distributional, and dynamic properties of individual driving behavior. Specifically:

1. Measures of central tendency and dispersion are calculated, including the mean and median speeds, the 10th, 25th, 75th, and 90th percentiles, maximum speed, standard deviation, and coefficient of variation. These metrics jointly describe the typical operating speed level, variability, and the presence of extreme driving conditions.
2. Distributional features are derived by partitioning the full range of speed into five predefined intervals—[0, 3) km/h (stopping), [3, 30) km/h (low), [30, 60) km/h (medium), [60, 90) km/h (high), and [90, 180] km/h (very high). The normalized occupancy probability within each interval is computed, providing a fine-grained view of how frequently drivers remain in low-speed congested states, cruise at medium speeds, or engage in high-speed operations.
3. Dynamic fluctuation features capture instantaneous changes in driving behavior using the first-order absolute differences between consecutive speed observations. The mean absolute variation, the 50th and 95th percentiles

of change amplitude, and the proportion of variations exceeding 10 km/h are computed. These indicators collectively describe driving smoothness, responsiveness to traffic conditions, and the frequency of sudden acceleration or deceleration events.

4. Uniformity metrics are quantified by computing the Shannon entropy of the speed distribution, which measures the regularity or irregularity of a driver's speed patterns and distinguishes monotonic cruising from highly volatile driving.

To strictly validate the optimal number of driving-style clusters, this study conducts a quantitative evaluation using silhouette analysis across a range of cluster counts (k=2-6). As illustrated in Figure 4, both K-Means and the Gaussian Mixture Model (GMM) exhibit peak silhouette scores at k=3, indicating an optimal balance between intra-cluster cohesion and inter-cluster separation. Notably, GMM achieves a significantly higher score of 0.72 compared to the 0.56 value obtained with K-Means at this threshold, underscoring its superior ability to capture the heterogeneous, non-spherical distributions inherent in real-world driving data. For k values greater than 3, silhouette scores decline sharply in both methods, suggesting that increasing the cluster count merely fragments coherent behavioral groups rather than revealing meaningful new patterns.

Supported by this evidence, the study adopts GMM with k = 3 as the final classification framework. Consequently, feature vectors are aggregated into a vehicle-by-feature matrix and partitioned using this probabilistic method [24]. This approach allows for soft assignments that account for latent heterogeneity, ultimately classifying each vehicle into one of three distinct archetypes: conservative, moderate, or aggressive. These categories form the analytical foundation for the subsequent behavioral modeling and comparative studies. To explicitly characterize the kinematic differences among the identified clusters, Figure 5 compares the centroids of five representative features: mean speed, standard deviation of speed, maximum speed, mean acceleration,

FIGURE 4 Silhouette Score as a function of the number of clusters (k) for K-Means and GMM.

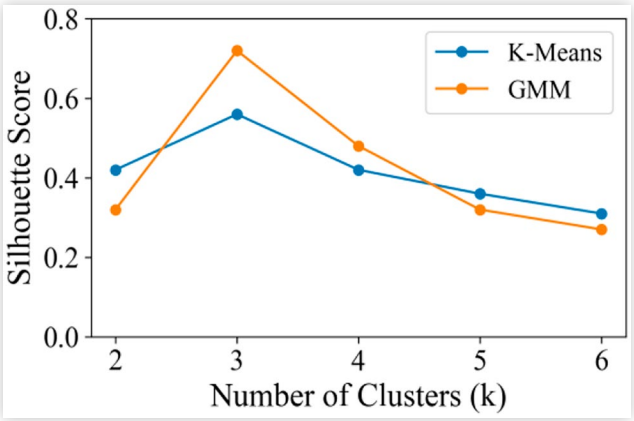

FIGURE 5 Comparison of statistical feature centroids across the three identified driving style clusters.

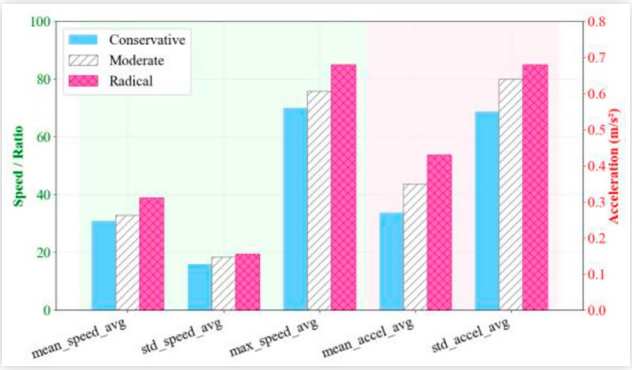

and standard deviation of acceleration. A clear monotonic increase in dynamic intensity is observed from the 'Conservative' to the 'Radical' group. These distinct feature distributions validate the effectiveness of the clustering framework in capturing heterogeneous driving behaviors.

Battery SOH Estimation and Degradation Profiling

Following the driving-style clustering, this study uses processed charging segment data to estimate and statistically smooth each vehicle's SOH [25]. The raw vehicular data, after rigorous preprocessing, are segmented into stable, qualified charging events. These segments serve as the foundation for extracting the battery's SOH. The extracted data are then used to construct and train the predictive degradation model.

Reference SOH Calculation The SOH is the key metric that defines the battery's current performance. Quantitatively, it is typically defined as the ratio of the battery's current maximum available capacity (Q_{now}) to its initial factory-rated capacity (Q_{rated}). Since the Q_{now} cannot be directly measured in real-world vehicle operation, it must be calculated indirectly from recorded telemetry data, specifically the charging current (I) and the SOC. The reference SOH is calculated using the following constitutive equations, as widely established in Equation (1),

$$SOH = \frac{Q_{now}}{Q_{rated}} \times 100\% \quad (1)$$

where Q_{rated} is the initial nominal capacity of the battery, and Q_{now} is the current maximum available capacity. The Q_{now} is estimated during a charging cycle by combining Coulomb counting with the observed change in SOC, as expressed by Equation (2),

$$Q_{now} = \frac{\int_{t_{start}}^{t_{end}} I(t)\,dt}{SOC_{end} - SOC_{start}} = \frac{\int_{t_{start}}^{t_{end}} I(t)\,dt}{DOC} \quad (2)$$

where I(t) represents the instantaneous charging current, $\int_{t_{start}}^{t_{end}} I(t)dt$ is the total ampere-hours delivered to the battery during the segment, and SOC_{start} and SOC_{end} are the batteries' SOC at the beginning and end of the charging segment, respectively. In addition, a critical parameter in this calculation is the Depth-of-Charge (DOC), defined as $DOC = SOC_{end} - SOC_{start}$.

To ensure the robustness and accuracy of the calculated Q values, this study implements a stringent filtering criterion: only charging segments with a DOC greater than 20% are retained. Segments with lower DOC are intentionally excluded because cumulative errors from current sensor quantization noise and SOC estimation drift can introduce significant fluctuations and larger relative errors in the calculated capacity value. Conversely, while maximizing DOC enhances precision, an overly aggressive threshold would severely reduce the number of available data points, thereby diminishing the study's statistical significance.

Battery SOH Label Preprocessing Using the steps above, this study calculates the SOH labels for each vehicle it collects. However, the calculated SOH values inherently exhibit substantial noise due to multiple factors, including sensor measurement precision, sampling frequency limitations, and signal interference during data transmission. To derive a robust and reliable degradation trajectory essential for model training, the raw SOH labels underwent a two-stage preprocessing procedure [26].

To effectively eliminate anomalous data points that could unduly bias the overall capacity curve, this study initially applies the Z-score filtering algorithm to the calculated capacity data. This algorithm identifies and removes data points that deviate significantly from the mean, thereby preserving the core data characteristics while mitigating the influence of extreme values on the subsequent analysis. The standardized score (Z_i) for each data point is calculated through Equation (3),

$$Z_i = \frac{x_i - \mu}{\sigma} \tag{3}$$

where x_i is the original capacity value of the i_{th} data point, μ is the mean of the capacity data, and σ is the standard deviation of the capacity data. In this study, a widely accepted rule is adopted: a data point is classified as an outlier and subsequently removed if $|Z_i|>2$.

Even after the Z-score filtering, the SOH labels continued to exhibit considerably high-frequency fluctuations. For practical real-world applications in EVs, the precise SOH value for each charging event is less critical than understanding and predicting the overall long-term degradation trend [27]. Instantaneous SOH variations are often stochastic, resulting from transient influences such as ambient temperature, immediate charging protocol, and individual driving habits, and are not reflective of underlying electrochemical aging.

FIGURE 6 Reference labels for the SOH of bicycles after data processing. The blue dots represent the inner-layer data retained after outlier removal, the gray dots represent the excluded outliers, and the red curve represents the LOWESS-fitted trend.

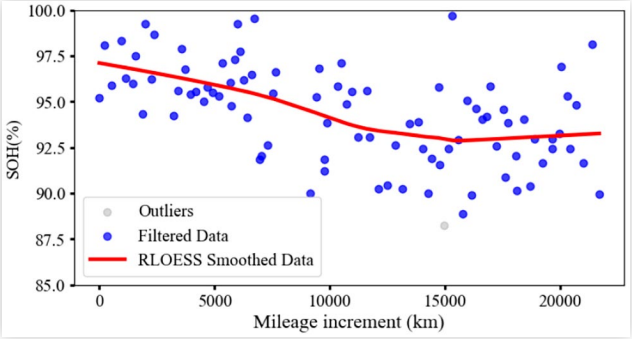

Therefore, to qualitatively describe and capture the fundamental, long-term degradation trajectory, the Locally Weighted Scatterplot Smoothing LOWESS algorithm is utilized for data smoothing [28], as described in Equation (4),

$$\widehat{SOH}(x) = \sum_i w_i(x) SOH_i \tag{4}$$

Where, $\widehat{SOH}(x)$ is computed as the weighted sum of all observed SOH_i values. LOWESS is a non-parametric regression technique that produces a smooth curve by fitting simple polynomial models to localized subsets of the data. In addition, $w_i(x)$ is defined by a tricube kernel through Equation (5),

$$w_i(x) = \left(1 - \left|\frac{x_i - x}{h}\right|^3\right)^3, \quad |x_i - x| < h \tag{5}$$

where h is the smoothing bandwidth (set as 0.6 times the data range). This combination of statistical filtering and local regression provides a stable, physically meaningful representation of degradation evolution.

As shown in Figure 6, the resulting SOH trajectories provide a quantitative foundation for linking driving and charging behaviors to long-term battery health outcomes.

Results and Discussions

After the above cleaning and processing of the raw data, this section presents the empirical analysis results derived from the integrated dataset described in the previous sections. The results are organized into three complementary analytical dimensions. First, the evolution of the SOH is compared under three predefined driving styles—conservative, moderate, and aggressive—to illuminate the behavioral dependence of degradation patterns.

Second, under controlled mileage and consistent driving-style conditions, the relationships between SOH and both fast-charging frequency and deep charge–discharge frequency are examined, providing real-world validation of SOH deterioration under different behavioral patterns.

SOH Degeneration under Different Driving Styles

To quantify behavioral differences in battery degradation among EV users, the analysis estimates a distance-normalized degradation rate—ΔSOH per 20,000 km—for each driving-style cohort, as shown in Figure 7. Median degradation increases monotonically with driving aggressiveness: conservative users exhibit the smallest decline, at approximately −0.9% per 20,000 km, followed by moderate users, at approximately −2.2%, and radical users, at approximately −4.0%. Holding external operating conditions constant, the radical cohort exhibits an 81% higher median degradation rate than the moderate cohort, indicating significantly faster capacity fades under aggressive driving conditions. The ordered separation of medians across cohorts, together with the widening dispersion visible in Figure 7, provides consistent evidence that driving style is a first-order determinant of battery SOH trajectories. In effect, the systematic progression from conservative to radical styles maps onto progressively steeper ΔSOH/20,000-km slopes, establishing a clear dose–response relationship between driving aggressiveness and long-term deterioration in battery health. The significant increase in degradation rate is consistent with previous research [16,17], which confirms that aggressive driving behavior can cause greater damage to vehicle battery SOH.

Relationship Between Deep Charge-Discharge Frequency and SOH

Irreversible degradation associated with deep cycling in lithium-ion batteries is well documented, arising primarily from mechanical stress in electrode lattices and intensified electrolyte side reactions at extreme SOC [29].

FIGURE 7 Distribution of EV battery SOH degradation rates in 20,000 km by driving style.

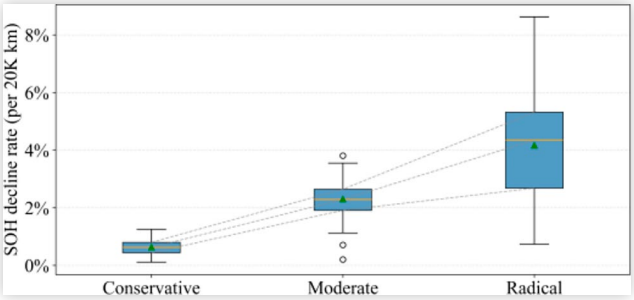

FIGURE 8 Box plot of SOH versus deep charge-discharge frequency, under conditions of equal mileage and identical fast-charging counts.

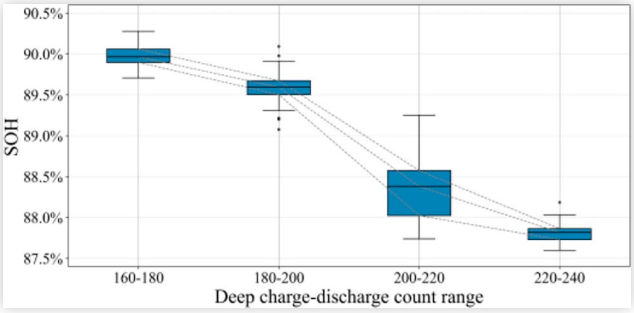

Building on this evidence, the present analysis treats the cumulative count of deep charge–discharge cycles as a key explanatory variable, where deep discharge is defined as operation below SOC ≤ 15% and deep charge as SOC ≥ 95%. To isolate behavioral effects, vehicles are compared within common strata of total mileage and fast-charging frequency. It is important to note that the specific frequency intervals (e.g., 160–180 to 220–240 cycles) were not arbitrarily chosen as user categories. Instead, they represent the common data-dense strata shared by the studied vehicles within the same mileage range. By selecting these overlapping intervals, we ensure a strict 'ceteris paribus' comparison, isolating the marginal effect of deep cycling while neutralizing the confounding impact of total distance traveled and driving styles. Within each stratum, deep-cycle counts are binned into equal-width intervals (20-cycle bins: 160–180, 180–200, 200–220, 220–240), and the resulting SOH distributions are contrasted using box plots, as shown in Figure 8.

The SOH central tendency declines approximately monotonically with increasing deep-cycle intensity: median SOH decreases from around 90% in the 160–180 bin to around 87.7–88.0% in the 220–240 bin. On a marginal basis, each additional 20 deep cycles is associated with a drop in median SOH of around 0.6–0.8%, corresponding to a cumulative reduction of around 2.0–2.3% across the studied range. While occasional outliers are observed, the ordered separation of medians and the consistent downward shift in the interquartile ranges indicate a clear dose–response relationship between deep-cycling frequency and capacity fade. This trend aligns with degradation patterns observed in cycle-life testing [30]. It confirms that frequent exposure to extreme SOC limits below 15% and above 95% accelerates the loss of active lithium inventory, even under varied real-world operating conditions. When controlled for mileage and fast-charging variations, these field observations corroborate established mechanistic pathways triggered at extreme SOCs, such as amplified particle cracking due to volume changes, SEI thickening, and parasitic reactions. Consequently, these findings underscore the importance of minimizing deep cycling as a critical strategy for SOH preservation.

Relationship Between Fast Charging Frequency and SOH

The study examines the association between fast-charging frequency and EV battery SOH under real-world operating conditions. Because elevated charge currents and the attendant thermal load can accelerate degradation mechanisms, the cumulative count of fast-charging events is defined as a key explanatory variable for this phenomenon. A fast-charging event is operationally defined as any charging session with average power over 35 kW. To isolate its effect, vehicles are compared within common strata of total mileage and deep charge–discharge frequency. Within each stratum, the number of fast-charge events is grouped into equal-width bins of 30 events — frequencies of fast-charging at 90-120, frequencies of fast-charging at 120-150, and frequencies of fast-charging at 150-180—and SOH distributions are contrasted using box plots, as shown in Figure 9. These specific bins (90–120, 120–150, 150–180) were identified as the common operational domains across the fleet's dataset. While different driving styles may naturally exhibit different charging preferences, comparing SOH within these unified intervals is essential to decouple the impact of charging intensity from the driving behavior itself. This approach allows us to quantify the SOH cost of increased fast charging for any given vehicle profile.

Results show a clear, monotonic decline in battery SOH with increasing fast-charging frequency. The median SOH is highest in the 90–120 bin, at approximately 90.2%. It decreases from 120–150 to around 89.4% and further declines from 150–180 to approximately 88.1%. Moving from 90–120 to 150–180 fast-charge events corresponds to an absolute reduction of approximately 2.1% in median SOH over the same mileage and deep-cycling conditions. The ordered separation of the median and the tightening of the upper quantile indicate a dose-response relationship, where more frequent exposure to high-power charging is associated with lower systemic battery health. Although not strictly causal, these on-site results are consistent with previous laboratory results [31] and emphasize the importance of managing fast charging intensity in lifespan-oriented charging strategies.

FIGURE 9 Box plot of SOH versus fast-charging frequency, under conditions of equal mileage and identical deep charge-discharge counts.

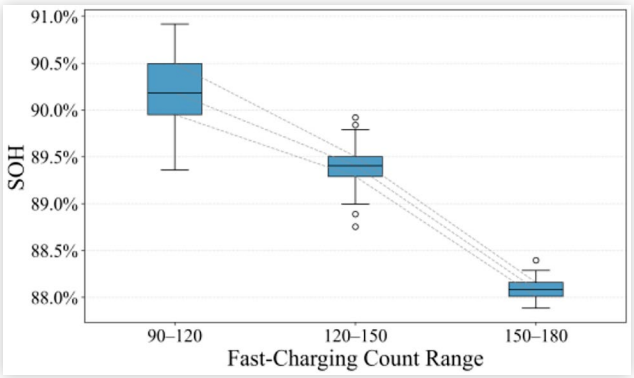

Conclusion

This study proposes a robust, data-driven framework that leverages large-scale, real-world operational data to quantify how user behavior drives EV battery degradation. Addressing a critical evidence gap between controlled laboratory findings and heterogeneous field conditions, this framework couples scalable telematics ingestion with multidimensional feature engineering to characterize both driving style and charging practices at the vehicle level. It then estimates SOH via charging-segment analysis—chosen for its smoother current trajectories and superior identifiability—before evaluating how behavioral heterogeneity shapes degradation dynamics under rigorous stratification by mileage and cycling intensity to mitigate confounding. The innovation lies in (i) distance-normalized, cohort-wise degradation metrics that enable interpretable effect sizes; (ii) joint treatment of driving aggressiveness, deep cycling, and fast-charging frequency within a unified field pipeline; and (iii) a design that is deployment-ready for fleet operations and personalized battery-management strategies. Empirical results not only corroborate electro-thermal mechanisms reported in laboratory studies but also provide statistically grounded, magnitude-specific estimates of behavior-linked capacity fade at scale. The framework thus delivers both external validity and operational relevance, informing warranty risk, residual-value modeling, infrastructure planning, and adaptive user feedback. The principal contributions and findings are as follows.

1. Driving aggressiveness and SOH decline. A clear association is established between driving aggressiveness and distance-normalized SOH loss. Relative to the moderate cohort, the radical cohort—characterized by higher magnitudes and frequencies of acceleration and deceleration—exhibits a median degradation rate approximately 81% higher per 20,000 km. This effect is consistent with elevated electro-thermal stress from higher root-mean-square current, which intensifies parasitic reactions (e.g., lithium plating) and accelerates irreversible capacity loss.
2. Deep cycling intensity. Holding the driving range and fast-charging frequency constant, increasing the number of deep charge–discharge cycles from 160–180 to 220–240 is associated with an additional reduction of around 2.0%–2.3% in median SOH, which is approximately 0.6%–0.8% per additional 20 deep cycles. Operation at very low, less than 15%, or very high SOC, over 95%, likely amplifies structural stress and electrolyte side reactions in electrode materials, accelerating degradation.
3. Fast-charging frequency. At fixed mileage and deep-cycling frequency, increasing fast-charge

events from 90–120 to 150–180 corresponds to an around 2.1% reduction in median SOH. This field evidence is consistent with accelerated degradation under high current and elevated temperature typical of fast charging, highlighting fast-charge
intensity as a salient behavioral risk factor.

However, some limitations of this study should be noted. First, the empirical analysis relies on high-frequency telematics data from seven specific battery EVs of the same model. While the dataset is extensive in temporal resolution (totaling ~15 million records), the concentration on a specific vehicle model and a limited number of unique vehicles suggests that future work should expand to broader fleets with diverse battery chemistries to verify the generalizability of these behavioral thresholds. Second, this study primarily focuses on user-controllable behaviors; future research should further integrate environmental covariates, such as seasonal temperature variations, into physics-informed machine-learning prognostics to improve personalized remaining-useful-life estimation.

Collectively, these results carry practical implications for the sustainable operation of EV fleets. The methodology provides a foundation for personalized battery management system strategies, including adaptive charging protocols that modulate charge power based on inferred driving styles, and real-time feedback systems that encourage users to adopt energy-efficient, battery-preserving behaviors. Specifically, based on the observed impact of charging intensity, limiting the percentage of fast-charging sessions is crucial for high-risk users. The findings suggest that shifting the charging mix towards a higher proportion of slow charging, particularly by avoiding fast charging when the battery is already under thermal stress or at high SOC levels, can significantly mitigate SOH decline. For fleet operators, this implies that capping the frequency of fast-charging events—keeping them below a critical threshold relative to total charging usage—serves as an effective, data-backed lever to extend battery longevity.

References

1. Samancıoğlu, U.E., Göçmen, S., Madani, S.S., Ziebert, C. et al., "An experimental and Comparative Study on Passive and Active PCM Cooling of a Battery With/Out Copper Mesh and Investigation of PCM Mixtures," *Journal of Energy Storage* 103 (2024): 114262.
2. Liu, T., Qi, H., and Ou, S., "Assessing the Energy Consumption Impact of Intelligent Driving Technologies on Electric Vehicles: A Comprehensive Review," SAE Technical Paper 2025-01-8598 (2025), https://doi.org/10.4271/2025-01-8598.
3. "*Global EV Outlook 2025*," accessed October 6, 2025, Trends in electric Car Markets – Global EV Outlook 2025 – Analysis - IEA
4. Geng, Z. and Thiringer, T., "In Situ Key Aging Parameter Determination of a Vehicle Battery using Only CAN Signals in Commercial Vehicles," *Applied Energy* 314 (2022): 118932.
5. Nakano, K., Vögler, S., and Tanaka, K., "Advancing State of Health Estimation for Electric Vehicles: Transformer-Based Approach Leveraging Real-World Data," *Advances in Applied Energy* 16 (2024): 100188, doi:10.1016/j.adapen.2024.100188.
6. Demirci, O., Taskin, S., Schaltz, E., and Demirci, B.A., "Review of Battery State Estimation Methods for Electric Vehicles-Part II: SOH Estimation," *Journal of Energy Storage* 96 (2024): 112703, doi:10.1016/j.est.2024.112703.
7. Kleiner, J., Stuckenberger, M., Komsiyska, L., and Endisch, C., "Advanced Monitoring and Prediction of the Thermal State of Intelligent Battery Cells in Electric Vehicles by Physics-Based and Data-Driven Modeling," *Batteries* 7, no. 2 (2021): 31.
8. Demirci, O., Taskin, S., Schaltz, E., and Demirci, B.A., "Review of Battery State Estimation Methods for Electric Vehicles-Part II: SOH Estimation," *Journal of Energy Storage* 96 (2024): 112703.
9. Koroma, M.S., Costa, D., Philippot, M., Cardellini, G. et al., "Life Cycle Assessment of Battery Electric Vehicles: Implications of Future Electricity Mix and Different Battery End-Of-Life Management," *Science of The Total Environment* 831 (2022): 154859.
10. Zhao, J., Ling, H., Wang, J., Burke, A.F. et al., "Data-Driven Prediction of Battery Failure for Electric Vehicles," *Iscience* 25, no. 4 (2022).
11. Liu, H., Chen, F., Tong, Y., Wang, Z. et al., "Impacts of Driving Conditions on EV Battery Pack Life Cycle," *World Electric Vehicle Journal* 11, no. 1 (2020): 17.
12. Alsharif, A., "Empirical Analysis of Electric Vehicle Battery Performance, Charging Behaviour, and Degradation: A Meta-Study of Published Experimental Results," *(ALBAHIT) Albahit Journal of Applied Sciences* (2025): 1-8.
13. Technology Networks, "Real-World Data Shows EV Batteries Outperform Lab Predictions," 2024. Available at: https://www.technologynetworks.com/applied-sciences/news/real-world-data-shows-ev-batteries-outperform-lab-predictions-394125.
14. Zhang, C., Wang, J., Zhang, L., Zhang, W. et al., "Decoding Battery Aging in Fast-Charging Electric Vehicles: An Advanced SOH Estimation Framework using Real-World Field Data," *Energy Storage Materials* 78 (2025): 104236.
15. Pozzato, G., Allam, A., Pulvirenti, L., Negoita, G.A. et al., "Analysis and Key Findings from Real-World Electric Vehicle Field Data," *Joule* 7, no. 9 (2023): 2035-2053.
16. Hu, L., Chen, J., Huang, J., Tian, Q. et al., "Study on the Impact of Driving Styles on EV Battery Pack SOC Inconsistency based on Real Urban Driving Data," *Applied Energy* 399 (2025): 126426.
17. Zhao, J., Ling, H., Wang, J., Burke, A.F. et al., "Data-Driven Prediction of Battery Failure for Electric Vehicles," *Iscience* 25, no. 4 (2022), doi:10.1016/j.isci.2022.103784.
18. Chou, K.S., Aguiari, D., Tse, R., Tang, S.-K. et al., "Impact Evaluation of Driving Style on Electric Vehicle Battery based on Field Testing Result," in *IEEE 20th Consumer*

Communications & Networking Conference (CCNC), 1143-1146, 2023.

19. Capasso, C., Iannucci, L., Sequino, L., Vaglieco, B.M. et al., "Driving Style Effects on Road EV Battery Performance and Remaining Useful Life," SAE Technical Paper 2023-24-0169 (2023), https://doi.org/10.4271/2023-24-0169.
20. Etxandi-Santolaya, M., Mora-Pous, A., Canals Casals, L., Corchero, C. et al., "Quantifying the Impact of Battery Degradation in Electric Vehicle Driving through Key Performance Indicators," *Batteries* 10, no. 3 (2024): 103.
21. Gonzalez-Rodriguez, P.S., Lozoya-Santos, J.J., Gonzalez-Hernandez, H.G., Felix-Herran, L.C. et al., "Challenges and Opportunities for Extending Battery Pack Life Using New Algorithms and Techniques for Battery Electric Vehicles," *World Electric Vehicle Journal* 16, no. 8 (2025): 442.
22. Wen, S., Lin, N., Huang, S., Li, X. et al., "Lithium Battery State of Health Estimation using Real-World Vehicle Data and an Interpretable Hybrid Framework," *Journal of Energy Storage* 96 (2024): 112623.
23. Lin, M., Wu, D., Chen, S., Meng, J. et al., "Battery Health Prognosis based on Sliding Window Sampling of Charging Curves and Independently Recurrent Neural Network," *IEEE Transactions on Instrumentation and Measurement* 73 (2024): 1-9.
24. Jurecki, R.S. and Stańczyk, T.L., "A Methodology for Evaluating Driving Styles in Various Road Conditions," *Energies* 14, no. 12 (2021): 3570.
25. Jing, H., Hu, J., Ou, S., Lv, Z. et al., "Scalable and Generalizable Deep Learning for Battery State of Health Estimation in On-Road Electric Vehicles," *Journal of Energy Chemistry* (2025).
26. Wen, S., Lin, N., Huang, S., Li, X. et al., "Lithium Battery State of Health Estimation using Real-World Vehicle Data and an Interpretable Hybrid Framework," *Journal of Energy Storage* 96 (2024): 112623, doi:10.1016/j.est.2024.112623.
27. Deng, Z., Xu, L., Liu, H., Hu, X. et al., "Prognostics of Battery Capacity based on Charging Data and Data-Driven Methods for On-Road Vehicles," *Applied Energy* 339 (2023): 120954, doi:10.1016/j.apenergy.2023.120954.
28. Jing, H., Hu, J., Ou, S., Qian, X. et al., "A Data-Driven and Physics-Based Model for Assessing Real-World Usage Behavior Impacts on Electric Vehicle Battery Life," *Journal of Energy Storage* 144 (2026): 119680, doi:10.1016/j.est.2025.119680.
29. Sagaria, S., van der Kam, M., and Boström, T., "Vehicle-To-Grid Impact on Battery Degradation and Estimation of V2G Economic Compensation," *Applied Energy*, 377: 124546, 2025.
30. Zhou, H., Yang, Y., Zhang, Z., Wang, W. et al., "Charge and Discharge Strategies of Lithium-Ion Battery Based on Electrochemical-Mechanical-Thermal Coupling Aging Model," *Journal of Energy Storage* 99 (2024): 113484.
31. Kumar, K., Rithvik, G., Mittal, G., Arya, R. et al., "Impact of Fast Charging and Low-Temperature Cycling on Lithium-Ion Battery Health: A Comparative Analysis," *Journal of Energy Storage* 94 (2024): 112580.

Contact Information

Shiqi(Shawn) Ou
sou@scut.edu.cn; oushiqi@pazhoulab.cn
Phone number: +86-020-81181684
Mailing address:
1. South China University of Technology, School of Future Technology, 777 Xingye Ave East, Panyu District, Guangzhou, Guangdong, 511442, China
2. Guangdong Artificial Intelligence and Digital Economy Laboratory (Guangzhou), 70 Yuean Road, Haizhou District, Guangzhou, Guangdong 510335, China

Acknowledgments

This work is supported by the National Key Research and Development Program of China (2024YFE0115800) and the Department of Science and Technology of Guangdong Province (2023ZT10L145). All opinions expressed in this paper are the authors' and do not necessarily reflect the policies and views of the sponsor.

ISSN 0148-7191